

Prompt emission of nucleon jets in time-dependent Hartree-Fock collisions

K. R. S. Devi

*W. K. Kellogg Radiation Laboratory, California Institute of Technology,
Pasadena, California 91125*

M. R. Strayer

*A. W. Wright Nuclear Structure Laboratory and Department of Physics, Yale University,
New Haven, Connecticut 06511*

K. T. R. Davies

Physics Division, Oak Ridge National Laboratory, Oak Ridge, Tennessee 37830

S. E. Koonin

*W. K. Kellogg Radiation Laboratory, California Institute of Technology,
Pasadena, California 91125*

A. K. Dhar

*Science Research Council, Daresbury Laboratory, Warrington Wa 4 4ad, United Kingdom
(Received 29 May 1981)*

The prompt emission of fast nucleon jets is calculated in the time-dependent Hartree-Fock approximation for $^{16}\text{O} + ^{93}\text{Nb}$ collisions at $E_{\text{lab}} = 204$ MeV. The emission time is independent of the entrance channel angular momentum and is approximately equal to the time needed for projectile nucleons to traverse the target without interacting. The mean laboratory velocity, scattering angle, and particle number of the jet are calculated and interpreted in terms of a zero temperature Fermi gas model. The neutron multiplicity in the jet in coincidence with deep inelastic scattering is found to be consistent with recent experimental measurements.

[NUCLEAR REACTIONS $^{16}\text{O} + ^{93}\text{Nb}$ at $E_{\text{lab}} = 204$ MeV in the time
dependent Hartree-Fock approximation. Single nucleon emission with
fusion and deep inelastic scattering.]

The phenomenon of light particle emission in heavy ion collisions can provide useful information about the various phases of these reactions. A variety of light particles are usually emitted, both during the collision itself and after the collision from the final fragments. These processes exist at virtually all bombarding energies above the Coulomb barrier, for appropriate projectile-target combinations, and are produced by several different mechanisms. High-energy single nucleon spectra have been measured in coincidence with both fused^{1,2} and deeply inelastic³ final states for several systems. These data have been analyzed using both local equilibrium and nonequilibrium macroscopic⁴⁻⁹ and microscopic¹⁰ models. Energy and

angle differential cross sections can be calculated in both pictures and seem to give similar results, even though they are based on very different physical assumptions. In the present study we present an analysis of the emission of fast nucleon jets observed in time-dependent Hartree-Fock (TDHF) calculations of $^{16}\text{O} + ^{93}\text{Nb}$ collisions at $E_{\text{lab}} = 204$ MeV. Our work addresses such basic questions as the time scale of emission, the composition of the jet, the angular focusing of the jet into the forward direction, and the jet's mean velocity.

The evolution to a final state in the TDHF approximation containing several fragments is not unexpected, since TDHF is a fully microscopic theory maintaining a separate wave function for

each nucleon. Multifragment final states were first observed in TDHF calculations of induced fission.¹¹ In studies of $^{88}\text{Kr} + ^{139}\text{La}$ at an incident energy of 710 MeV (Ref. 12) and $^{130}\text{Xe} + ^{209}\text{Bi}$ at 1130 MeV (Ref. 13) it was found that certain deep inelastic trajectories favor breakup into three fragments rather than two. For these events the collective field of the heavy fragments forces the neck at scission to breakup, forming a particle of about mass four. This type of nonsequential fragmentation occurs after about 2.4×10^{-21} s, a time which is long compared to that for the projectile to pass the target without interacting. In contrast, the emission of nucleons in the $^{16}\text{O} + ^{93}\text{Nb}$ system occurs very quickly, at approximately equal to the characteristic time for the projectile to pass the target without interacting. The number of fast nucleons is small and consists of localized "jets" of matter having a density about 1–2% of the central nuclear density. Fast jets of low density nucleons exhibiting these characteristics have also been observed in TDHF collisions of $^{12}\text{C} + ^{197}\text{Au}$ (Ref. 10) at much higher energies and also in one dimensional colliding slab studies.^{14,15} The matter in the jet is associated almost exclusively with those single particle wave functions initially localized in the projectile. The average velocity, scattering angle, and average number of particles in the jet are obtained as functions of the entrance channel angular momentum and are interpreted in terms of a Fermi gas model. This accounts qualitatively for the behavior of the TDHF jets, with the exception of the increase in their average velocity with increasing angular momentum.

The $^{16}\text{O} + ^{93}\text{Nb}$ reaction has been previously studied experimentally,⁹ and the emission of nonequilibrium neutrons in this system is well established. The neutron multiplicity measured in coincidence with the deep inelastic fragments is $M_n = 0.15 \pm 0.05$. In an earlier TDHF study¹⁶ of this system, using the frozen approximation, an anomalous behavior of the rms radius as a function of time was observed for angular momenta which correspond to fusion. We found that, for short times, the radius undergoes several oscillations, a feature normally seen in TDHF fusion¹⁷ studies. However, after about 2×10^{-21} s the radius dramatically increases in value, although explicit plots of the density contours show that the system maintains a single coalesced shape.¹⁶ Analysis now shows that this behavior is due to a shift of the center of mass resulting from multiple recoil effects. Early in the collision ($\approx 0.5 \times 10^{-21}$ s) there is the emission of a

jet which rapidly strikes the wall of the mesh and thereafter continues to bounce around in the model space, each collision with the wall causing a recoil of the center of mass.

Figure 1 displays density contour plots for entrance channel angular momentum $l=0$ and $l=33$ at times 0.47 and 0.50 (in units of 10^{-21} s). The left hand plot shows the matter density contours whose values are greater than 10% of the central density, ρ_0 ($\approx 0.15 \text{ fm}^{-3}$). The right hand plot shows the neutron density range between 1% and 10% of ρ_0 (neutron skin). Note that a small jet of neutrons has been ejected from the central density region, predominantly in the incident beam direction (z direction). Jets of protons, although not shown, are similarly emitted during the collision. A complete analysis of the composition and origin of the jet indicates that it is comprised of approxi-

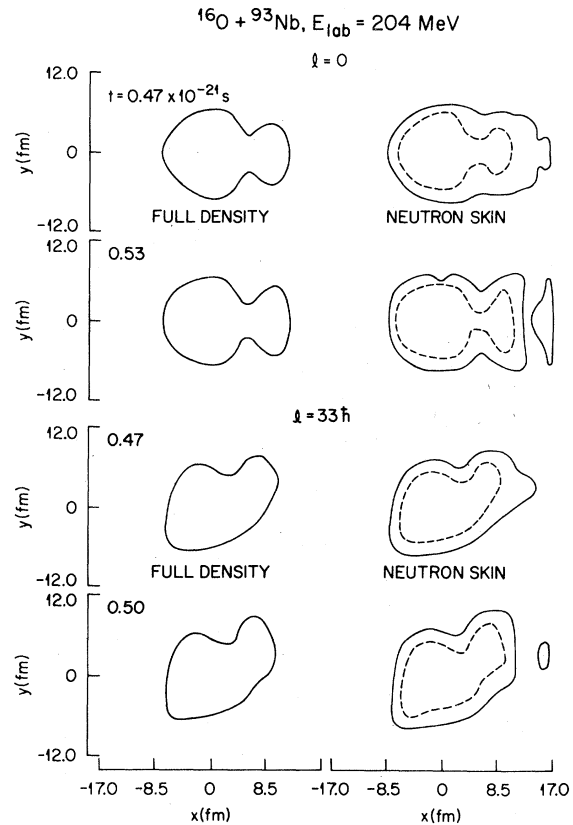


FIG. 1. Density contour plots in the reaction plane for the matter density $\rho > \rho_0/10$ (left), and the neutron skin density $\rho_0/10 > \rho > \rho_0/100$ (right) for two angular momenta and at two times. The solid curve on the left is the contour $\rho_0/10$. The solid curve on the right is the contour $\rho_0/100$, and the dashed curve on the right is the contour $\rho_0/10$. The central density is $\rho_0 \approx 0.15 \text{ fm}^{-3}$.

TABLE I. The minimum rms radius a_0 , the time at which the radius is a minimum, τ_0 , the time at which the jet is observed, τ_{jet} , the emission time of the jet, τ_{em} , and the fraction of the particles in the jet that are in orbits initially occupied in the projectile, f , for various entrance channel angular momenta l .

l (\hbar)	a_0 (fm)	τ_0 (10^{-21} s)	τ_{jet} (10^{-21} s)	τ_{em} (10^{-21} s)	f
0	4.657	0.227	0.400	0.173	0.75
10	4.668	0.233	0.393	0.160	0.930
20	4.691	0.240	0.400	0.160	0.920
30	4.720	0.247	0.400	0.153	0.90
40	4.757	0.247	0.420	0.173	0.88
50	4.800	0.267	0.467	0.200	0.80

mately equal parts of neutrons and protons from orbitals originally localized in the projectile.

Table I lists, for various values of the angular momentum l , the time when the rms radius reaches its minimum value (τ_0), the corresponding value of the rms radius (a_0), and the time when the jet is first emitted (τ_{jet}). Also tabulated is the emission time of the jet (τ_{em}), which is defined operationally as the difference between the time when the jet is first observed and the time when the overall system reaches its most compact shape. The fraction of the nucleons in the jet that were initially occupied as orbitals in the ^{16}O projectile, f , is also given. The $1s$ states typically account for only about 1% of this fraction, the remainder comes from the $1p$ states.

In Fig. 2 we plot (solid curves), as functions of l , the number of nucleons in the jet, $n_l = \langle \rho \rangle$ and v_l and θ_l , the magnitude of the velocity and angle of the jet in the lab frame. These velocities are obtained from the corresponding c.m. velocities given by

$$v_{\text{c.m.}} = \langle j \rangle / \langle \rho \rangle,$$

where ρ and j are the particle and current densities, respectively. The brackets pertain to expectation values in a restricted region of space surrounding the nucleon jet, which was chosen to be an area of $5 \times 35 \text{ fm}^2$. The quantities n_l and v_l were obtained by averaging $\langle \rho \rangle$ and $\langle j \rangle$ over a short interval (between the time of emission and the time when the particles in the jet collide with the boundary) during which they were found to be nearly constant. Because of the TDHF transparency, there is a problem in accurately calculating $\langle j \rangle$ and $\langle \rho \rangle$ for small values of l . The O-like ion "passes through" the Nb-like ion and follows closely behind the nucleon jet. Thus, it is difficult to nu-

merically isolate a region surrounding the jet due to contamination from the O-like ion. The mean

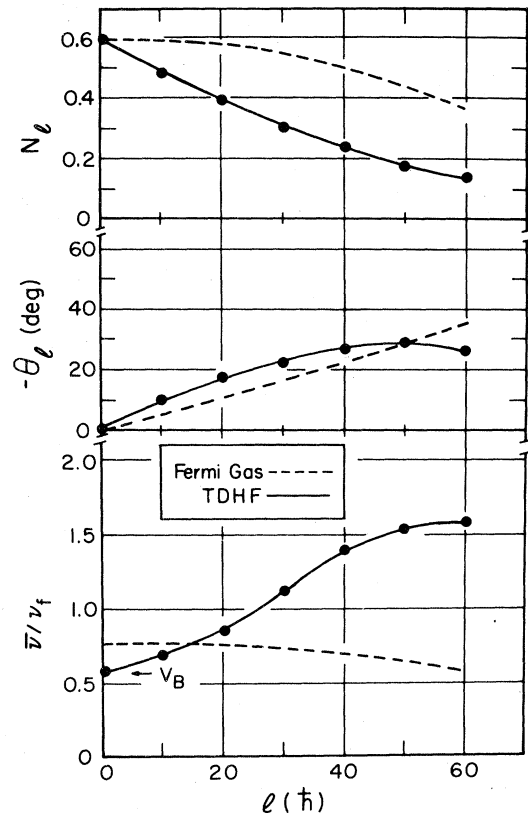


FIG. 2. The mean number of nucleons in the jet, the mean scattering angle, and velocity of the jet in the lab frame as functions of l from the TDHF calculations (solid circles; the lines are included to guide the eye) and from the Fermi gas model (dashed curves). The results for $l \geq 60$ are not plotted, since for these l the TDHF N values are extremely small and hence large errors are introduced in the calculations of velocities and scattering angles.

nucleon number is therefore only accurate to 50%. The velocity components of the jet are inherently more difficult to determine than the particle number. Their values are accurate to within a factor of 2. At all impact parameters the close proximity of the mesh boundary inhibits us from obtaining more reliable values.

The mean number of nucleons and jet velocity are quantities which characterize the average behavior of the jet. These are compared to the results obtained from a zero temperature Fermi gas model, the dashed curves in Fig 2. This model assumes that the projectile nucleons have the isotropic velocity distribution of a degenerate Fermi gas in the rest frame of the projectile. In the rest frame of the target, this velocity distribution is boosted by the relative motion of the two ions. The tangential velocity of the projectile particles, as they traverse the target potential, remain unaltered due to the conservation of angular momentum. Particles having a radial velocity greater than some threshold velocity v_t will be emitted. If T_{in} and T_{out} are the radial kinetic energies of the projectile particles inside the target and outside the target after emission, then from the conservation of energy,

$$T_{in} + W = T_{out} ,$$

where W is the potential energy in the target. Therefore, at threshold ($T_{out}=0$),

$$T_{in} = -W .$$

The potential W , which is generated by the target particles, can be obtained from the relation

$$t + W = B ,$$

where t is the kinetic energy of a target particle and B is the binding energy. Assuming, for simplicity, that t is approximately equal to the Fermi energy ϵ_f ,

$$T_{in} = \epsilon_f + |B|$$

and

$$v_t = v_f \left[1 + \frac{|B|}{\epsilon_f} \right]^{1/2} \approx 1.1 v_f .$$

Here we have used $B \approx 8$ MeV and $\epsilon_f \approx 38$ MeV, which corresponds to a Fermi velocity $v_f = 0.28c$ (c is the velocity of light). The probability for projectile nucleon emission for a head-on collision at $E_{lab} = 204$ MeV is

$$\left[\frac{\delta n}{n} \right]_{l=0} = 0.19 .$$

The probability is obtained assuming all projectile nucleons satisfying the above kinematical conditions will pass through the target. In more realistic macroscopic treatments the flux of outgoing particles will depend on the projectile-target overlap (window). Both the window area and orientation are generally functions of impact parameter and time⁴⁻⁶; however, for the purpose of qualitatively comparing the Fermi gas results with those of TDHF calculations, we have scaled the Fermi gas probability at $l=0$. Thus, our simple Fermi gas model does not employ a window. The results of the two calculations are compared in Fig. 2. We observe a qualitative agreement between the TDHF and model calculations for the mean particle number and the scattering angle. However, we observe that the TDHF jet velocity increases with increasing angular momentum by more than a factor of 2, whereas the Fermi gas jet velocity decreases by 30% over the same angular momentum range.

In TDHF calculations of jet emission at higher energies¹⁰ the mean velocity decreased as l increases, as in the Fermi gas model. We therefore conclude that our result might be spurious, arising from numerical uncertainty.

For the $^{16}\text{O} + ^{93}\text{Nb}$ collision at this energy, the upper and lower limits for fusion have been previously computed in TDHF using the two dimensional frozen approximation¹⁵

$$l_{<} = 31 ,$$

$$l_{>} = 75 ,$$

with inelastic scattering occurring for l below $l_{<}$ and above $l_{>}$. However, recent axially symmetric head-on calculations¹⁸ using the same interaction yield a fused final state at this energy. Although, in principle, the axially symmetric calculations for head-on collisions should yield the exact 3D results, the treatment of the initial static wave functions are different from the exact 3D case. Since currently no exact 3D calculations have been carried out for this system, the identification of the lower inelastic branch is uncertain. However, if we assume inelastic scattering for $l > l_{>}$, the calculated fast neutron multiplicity in coincidence with the deep inelastic scattering is

$$M_p(\text{TDHF}) = 0.19 .$$

The corresponding experimental value is

TABLE II. A comparison of the values of critical angular momentum l_c , mean jet velocity \bar{v} , emission time τ_{em} , and the total neutron multiplicity M_v , obtained from the Fermi gas model and from the TDHF calculations.

	TDHF	Fermi gas
$l_c (\hbar)$	70	82
\bar{v}/c	0.3	0.18
$\tau (10^{-21} \text{ s})$	0.2	
M_v	0.05	0.07

$$M_v(\text{expt}) = 0.15 \pm 0.05.$$

In both the TDHF and Fermi gas calculations there is a critical angular momentum l_c above which jetting is not observed. In Table II we display this critical angular momentum l_c , the mean time of emission, the mean velocity (averaged over the angular momenta), and the total multiplicity obtained from the TDHF and Fermi gas model calculations. The values obtained from the Fermi gas model follow closely the TDHF values except for the mean velocity (the possible reasons

for which are discussed earlier).

In summary, we have calculated the emission of fast nucleon jets in TDHF collisions of $^{16}\text{O} + ^{93}\text{Nb}$ at $E_{lab} = 204 \text{ MeV}$. We calculate an emission time of $\approx 0.2 \times 10^{-21} \text{ s}$ and a mean jet velocity $v_{lab}/c = 0.3$ in contrast to the incident beam velocity $v_B/c \approx 0.16$ and a Fermi velocity $v_f/c \approx 0.27$. A critical angular momentum above which the jetting is not observed is also determined, $l_c \approx 70$, and is partly responsible for the focusing of the jet into the forward direction. These results are qualitatively the same as those obtained with a simple Fermi gas model.

This work was supported in part by the National Science Foundation under contract PHY77-21602 at Caltech, the Division of Basic Energy Sciences, U.S. Department of Energy under Contract W-7405-ENG-26 with the Union Carbide Corporation, under Contract AC02-76ER03074 with Yale University, and the U. K. Science Research Council. The computations were performed on the Cray-1 computer at the SRC Daresbury Laboratory. S. E. Koonin is an Alfred P. Sloan Foundation Fellow.

- ¹H. C. Britt and A. R. Quinton, Phys. Rev. **124**, 877 (1961); J. Gallin, B. Gatty, D. Guerreau, C. Rousset, U. Schlotthauer-Voos, and X. Tarrago, Phys. Rev. C **9**, 1126 (1974).
- ²L. Westberg, D. G. Sarantites, D. C. Hensley, R. A. Dayras, M. L. Halbert, and J. H. Baker, Phys. Rev. C **18**, 796 (1978).
- ³A. Gavron, R. L. Ferguson, F. E. Obenshain, F. Plasil, G. R. Young, G. A. Petitt, K. A. Geoffroy, D. G. Sarantites, and C. F. Maguire (unpublished).
- ⁴J. P. Bondorf, J. N. De, G. Fai, A. O. T. Karvinen, and B. Jakobssons, Phys. Lett. **84B**, 163 (1979).
- ⁵J. P. Bondorf, J. N. De, G. Fai, A. O. T. Karvinen, B. Jakobsson, and J. Randrup, Nucl. Phys. **A333**, 285 (1980).
- ⁶M. C. Robel, Ph. D. thesis, Lawrence Berkeley Laboratory, 1979 (unpublished).
- ⁷R. Weiner and M. Westrom, Phys. Rev. Lett. **34**, 1523 (1975); Nucl. Phys. **A286**, 282 (1977).
- ⁸W. W. Morrison, S. K. Samadarr, D. Sperber, and M. Zielinska-Pfabe, Phys. Lett. **93B**, 379 (1980).
- ⁹S. I. A. Garpman, D. Sperber, and M. Zielinska-Pfabe, Phys. Lett. **90B**, 53 (1980).
- ¹⁰H. Stocker, R. Y. Cusson, J. A. Maruhn, and W. Greiner (unpublished).
- ¹¹J. W. Negele, S. E. Koonin, P. Moller, J. R. Nix, and A. J. Sierk, Phys. Rev. C **17**, 1098 (1978).
- ¹²K. T. R. Davies, K. R. S. Devi, and M. R. Strayer, Phys. Rev. C **20**, 1372 (1979).
- ¹³A. K. Dhar, B. S. Nilsson, K. T. R. Davies, and S. E. Koonin, Nucl. Phys. A (to be published).
- ¹⁴J. W. Negele, Proceedings of the Topical Conference on Heavy Ion Collisions, Fall Creek Falls, Tennessee, 1977 p. 73; P. Bonche, S. E. Koonin, and J. W. Negele, Phys. Rev. C **13**, 1226 (1976).
- ¹⁵H. S. Kohler, in *Time Dependent Hartree-Fock Methods*, edited by P. Bonche, B. Giraud, and P. Quentin (Editions de Physique, Orsay, France, 1979), p. 1.
- ¹⁶K. R. S. Devi, M. P. Strayer, J. M. Irvine, and K. T. R. Davies, Phys. Rev. C **23**, 1064 (1981).
- ¹⁷S. E. Koonin, K. T. R. Davies, V. Maruhn-Rezwani, H. Feldmeier, S. J. Krieger, and J. W. Negele, Phys. Rev. C **15**, 1359 (1977); K. T. R. Davies, K. R. Sandhya Devi, and M. R. Strayer, Phys. Rev. Lett. **44**, 23 (1980).
- ¹⁸A. K. Dhar, B. S. Nilsson, K. T. R. Davies, and J. P. Bondorf (unpublished).